Unsteady MHD Natural Convection Flow of Nanofluid in a Cavity Containing Adiabatic Obstacle with Heat Corners

A.M. Rashad[1], M.A. Mansour[2], Rama Subba Reddy Gorla[3,*], Sadia Siddiqa[4] and T. Salah[1,5]

[1]*Department of Mathematics, Aswan University, Faculty of Science, Aswan, 81528, Egypt*

[2]*Department of Mathematics, Assuit University, Faculty of Science, Assuit, Egypt*

[3]*Department of Mechanical Engineering, Cleveland State University, Cleveland, Ohio 44115 USA*

[4]*COMSATS University Islamabad, Attock Campus, Kamra Road, 43600, Attock, Pakistan*

[5]*Basic and Applied Sciences Department, College of Engineering and Technology, Arab Academy for Science & Technology and Maritime Transport (AASTMT), Aswan Branch, Egypt*

Abstract: Unsteady natural convection heat transfer of nanofluid within cavities with local heaters occurs in several engineering applications. Therefore, investigation of nanofluid flow and heat transfer processes in such systems has a considerable value for evolution of industry. In the current investigation, unsteady MHD natural convection flow of Cu-water nanofluid and heat transfer behavior in square cavity containing a centered adiabatic square block. The mathematical formulation part for present problem is presented in succeeding section. It has been found the size of the adiabatic obstacle influences the behavior of the nanofluid and conduction becomes dominant when size aspect ratio increases to 0.5. It is also noticed that angle of the applied magnetic field can maximize(minimum)the rate of heat transfer if applied in the stream-wise (normal) direction. The novelty of the present work is to consider cavity containing a centered adiabatic square block as well as unsteady effects in the natural convection of nanofluids.

Keywords: Magnetic field, Nanofluid, Natural convection, Cavity, Adiabatic block.

1. INTRODUCTION

Natural convection in several technologies finds an important place for engineering analysis. It has wide applications in engineering like solar applications, electronic industry, building applications, etc. The problem can be found for industrial boilers or ovens with porous materials. Also, boundaries of open or closed geometries can be non-linear. Also, convective heat transfer of nanofluids has been extensively investigated in recent years. Conventional heat transfer fluids such as water, oil and ethylene glycol have low thermal conductivity, which is an essential limitation in promoting the performance and the compactness of numerous engineering electronic devices. Thus, there is a strong need to develop advanced heat transfer fluids with substantially higher conductivities. With recently introduced nanofluids, which are the fluids with suspended solid particles of higher thermal conductivity such as metals within it, the aforementioned need has been overcome. Choi [1] is the pioneer author to employ the term “nanofluid”, which indicates the fluid with suspended nanoparticles. Eastmen *et al*. [2] indicated that nanofluids possess a substantially greater thermal conductivity than that of conventional ones. The experimental data results yield a much higher thermal conductivity than that predicted by these models. An alternative expression to predict the thermal conductivity of solid–liquid mixtures was proposed by Yu and Choi [3]. They claimed that a structural model of nanofluids might consist of a bulk liquid, solid nanoparticles and solid like nanolayers. The solid-like nanolayer acts as a thermal bridge between a solid nanoparticle and a bulk liquid.

Mansour *et al*. [4] investigated numerically the influence of thermal boundary conditions on thefree convection of Cu-water nanofluid inside enclosure. The results indicated that an enhancement in the Hartmann number results in a clear decrease in the rate of heat transfer and enhancement in Rayleigh number increases the nanofluid flow. Raza *et al.* [5] studied MHD flow and heat transfer of copper/water nanofluid in a semi porous channel with stretching walls. Azimi and Riazi [6] analyzed MHD copper/water nanofluid flow and heat transfer through a convergent-divergent channel. Rashad *et al*. [7] studied numerically the MHD natural convection of nanofluid inside cavity. It was found that as the increase in Hartmann number causes a decrease in the fluid motion and local Nusselt number along the heat source. Also, the average Nusselt number decreases by increase the heat source length whereas a strong enhancement in average Nusselt number obtained as the nanoparticle volume

*Address correspondence to this author at the Department of Mechanical Engineering, Cleveland State University, Cleveland, Ohio 44115 USA;
Tel: 1-216-687-2567; E-mail: r.gorla@yahoo.com

E-ISSN: 2409-5826/19

fraction increased. However, Some recent investigations on this topic can be mentioned in Refs. [8-10].

Motivated by the above studies and possible applications, we investigate numerically the unsteady MHD natural convection flow of Cu-water nanofluids and heat transfer behavior in square cavity containing a centered adiabatic square block. The novelty of the present work is to consider cavity containing a centered adiabatic square block as well as unsteady effects in the natural convection of nanofluids. The mathematical formulation part for present problem is presented in succeeding section. The numerical outcomes provide a detailed understanding of the impacts of the nanoparticle volume fraction, Hartman number, heat generation/absorption coefficient, heat sources length, respectively.

2. PROBLEM FORMULATION

A schematic diagram of the square cavity of length *H* filled with Cu-water nanofluid with internal heat generation is presented in Figure **1**. The cavity is containing an adiabatic square obstacle in the center of the cavity. An isothermal heat source with a constant hot temperature T_h is located on the effective segments of the upper and lower sides in the left corners of the cavity, and a heat sink with a constant cooled temperature of $T_c(T_h>T_c)$ are located on an effective segment of the left and right sides in right corners of the cavity, respectively. The other ineffective portions of the cavity's segments of sides walls are kept adiabatic. The length of the heat source which is the same as that of the heat sink is equal to *b*. The direction of the gravity force is downward and a magnetic field with strength β_O is applied on left side of the cavity with angle *Φ* along the positive horizontal direction. The cavity is filled with Copper-water nanofluid that is considered to be unsteady Newtonian, laminar, incompressible and exposed to internal heat generation at a uniform rate Q_0. In addition, the nanofluid is simulated as a single-phase homogeneous fluid. Thermophysical properties of the nanoparticles and the base liquid are gathered in Table **1**. The density variation in the nanofluid is approximated by the regular Boussinesq approximation. Therefore, governing equations can be given in dimensional mode as follows:

$$\frac{\partial u}{\partial x}+\frac{\partial v}{\partial y}=0 \tag{1}$$

$$\frac{\partial u}{\partial t}+u\frac{\partial u}{\partial x}+v\frac{\partial u}{\partial y}=-\frac{1}{\rho_{nf}}\frac{\partial p}{\partial x}+\nu_{nf}\left(\frac{\partial^2 u}{\partial x^2}+\frac{\partial^2 u}{\partial y^2}\right)+\frac{\sigma_n B_0^2}{\rho_{nf}} (v\sin\Phi\cos\Phi-u\sin^2\Phi) \tag{2}$$

$$\frac{\partial v}{\partial t}+u\frac{\partial v}{\partial x}+v\frac{\partial v}{\partial y}=-\frac{1}{\rho_{nf}}\frac{\partial p}{\partial y}+\nu_{nf}\left(\frac{\partial^2 v}{\partial x^2}+\frac{\partial^2 v}{\partial y^2}\right)+\frac{(\rho\beta)_{nf}}{\rho_{nf}}g(T-T_c)+\frac{\sigma_{nf}B_0^2}{\rho_{nf}}(u\sin\Phi\cos\Phi-v\cos^2\Phi) \tag{3}$$

$$\frac{\partial T}{\partial t}+u\frac{\partial T}{\partial x}+v\frac{\partial T}{\partial y}=\alpha_{nf}\left(\frac{\partial^2 T}{\partial x^2}+\frac{\partial^2 T}{\partial y^2}\right)+\frac{Q_0}{(\rho c_p)_{nf}}(T-T_c) \tag{4}$$

The appropriate initial and boundary conditions are as follows:

$t<0: u=v=T=0,\ 0\le x\le H,\ 0\le y\le H$

On the left wall:

$t\ge 0: x=0,\ u=v=0, \frac{\partial T}{\partial x}=0, b\le y\le H-b, T=T_h,$ otherwise.

On the right wall:

$t\ge 0: x=H,\ u=v=0,\ \frac{\partial T}{\partial x}=0,\ b\le y\le H-b, T=T_c,$ otherwise.

On the bottom wall:

$t\ge 0: y=0,\ u=v=0,\ T=T_h, 0\le x\le b, T=T_c, H-b\le x\le H,\ \frac{\partial T}{\partial y}=0$ otherwise.

On the top wall:

$$t\ge 0: y=H,\ u=v=0, T=T_h, 0\le x\le b, T=T_c, H-b\le x\le H, \frac{\partial T}{\partial y}=0 \text{ otherwise.} \tag{5}$$

In Eqs. (1)- (5), x and y are Cartesian coordinates measured along the horizontal and vertical walls of the cavity respectively, u and v are the velocity components along the x and y - axes respectively, T is the fluid temperature, *p* is the fluid pressure, *g* is the gravity acceleration. H is the length of the bottom wall, $(\rho\beta)_{nf}$ is a nanofluid buoyancy coefficient, σ_{nf} is the electrical conductivity of nanofluid β_O is the magnitude of the external magnetic field, Q_0 is the heat generation coefficient, anf is the effective nanofluid thermal diffusivity.

In the present investigation, we are adopting the relations which depend on the volume fraction of nanoparticles only and which were proven and used in many previous studies as follows:

The effective density of the nanofluid is given as (see Aminossadati and Ghasemi [11] and Khanfer *et al*. [12]):

$$\rho_{nf} = (1-\phi)\rho_f + \phi\rho_p \tag{6}$$

where ρ_f and ρ_p are the densities of the fluidand of the solid fractions respectively, φ is the solid volume fraction of the nanofluid. and the heat capacitance of the nanofluid given as:

$$(\rho c_p)_{nf} = (1-\phi)(\rho c_p)_f + \phi(\rho c_p)_p \tag{7}$$

The thermal expansion coefficient of the nanofluid can be determined by:

$$(\rho\beta)_{nf} = (1-\phi)(\rho\beta)_f + \phi(\rho\beta)_p \tag{8}$$

where β_f and β_p are the coefficients of thermal expansion of the fluid and of the solid fractions respectively. Thermal diffusivity α_{nf} of the nanofluid is defined by Abu-Nada and Chamkha [13 as:

$$\alpha_{nf} = \frac{k_{nf}}{(\rho c_p)_{nf}} \tag{9}$$

In Equation (9), k_{nf} is the thermal conductivity of the nanofluid which for spherical nanoparticles, according to the Maxwell-Garnetts model [14], is:

$$\frac{k_{nf}}{k_f} = \frac{(k_p + 2k_f) - 2\phi(k_f - k_p)}{(k_p + 2k_f) + \phi(k_f - k_p)} \tag{10}$$

The effective dynamic viscosity of the nanofluid based on the Brinkman model [15] is given by:

$$\mu_{nf} = \frac{\mu_f}{(1-\phi)^{2.5}} \tag{11}$$

where, μ_{nf} isnanofluid dynamic viscosity and the effective electrical conductivity of nanofluid was presented by Maxwell [14] as:

$$\frac{\sigma_{nf}}{\sigma_f} = 1 + \frac{3(\gamma-1)\phi}{(\gamma+2)-(\gamma-1)\phi} \tag{12}$$

where $\gamma = \dfrac{\sigma_p}{\sigma_f}$.

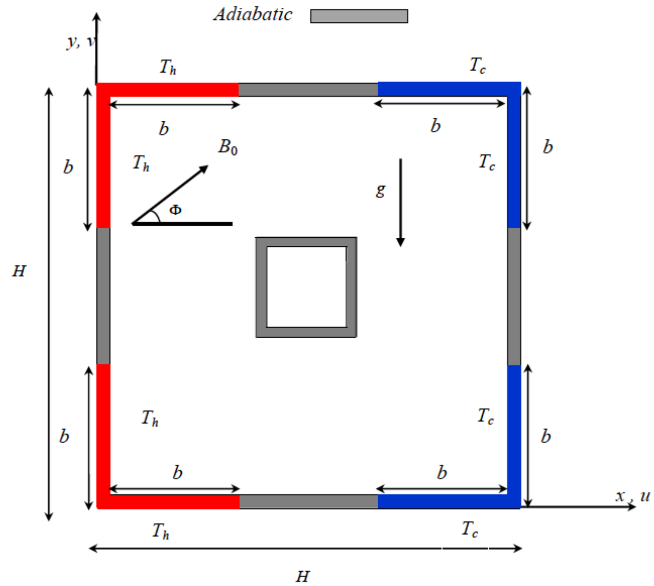

Figure 1: Schematic diagram and coordinate system.

Table 1: Thermophysical Properties of Water and Copper

Property	Water	Copper (Cu)
ρ	997.1	8933
C_p	4179	385
k	0.613	401
β	21×10^{-5}	1.67×10^{-5}
σ	0.05	$5.96\text{x}10^{7}$

Introducing the following dimensionless set:

$$X = \frac{x}{H},\ Y = \frac{y}{H},\ U = \frac{uH}{\alpha_f},\ V = \frac{vH}{\alpha_f},\ P = \frac{pH^2}{\rho_{nf}\alpha_f^2},\ \theta = \frac{T-T_c}{\Delta T},\ \Delta T = T_h - T_c,\ \tau = \frac{\alpha_f}{H^2}t \tag{13}$$

into Eqs. (1)-(5) yields the following dimensionless equations:

$$\frac{\partial U}{\partial X} + \frac{\partial V}{\partial Y} = 0 \tag{14}$$

$$\frac{\partial U}{\partial \tau} + U\frac{\partial U}{\partial X} + V\frac{\partial U}{\partial Y} = -\frac{\partial P}{\partial X} + \left(\frac{\mu_{nf}}{\rho_{nf}\alpha_f}\right)\Pr\left(\frac{\partial^2 U}{\partial X^2} + \frac{\partial^2 U}{\partial Y^2}\right) + \left(\frac{\mu_{nf}}{\rho_{nf}\alpha_f}\right)\left(\frac{\sigma_{nf}}{\sigma_f}\right)\Pr Ha^2(V\sin\Phi\cos\Phi - U\sin^2\Phi) \tag{15}$$

$$\frac{\partial V}{\partial \tau}+U\frac{\partial V}{\partial X}+V\frac{\partial V}{\partial Y}=-\frac{\partial P}{\partial Y}+\left(\frac{\mu_{nf}}{\rho_{nf}\alpha_f}\right)\Pr\left(\frac{\partial^2 V}{\partial X^2}+\frac{\partial^2 V}{\partial Y^2}\right)$$
$$+\frac{(\rho\beta)_{nf}}{\rho_{nf}\beta_f}Ra\Pr\theta-\left(\frac{\sigma_{nf}}{\sigma_f}\right)\left(\frac{\rho_f}{\rho_{nf}}\right)\Pr Ha^2(U\sin\Phi\cos\Phi-V\cos^2\Phi) \quad (16)$$

$$\frac{\partial \theta}{\partial \tau}+U\frac{\partial \theta}{\partial X}+V\frac{\partial \theta}{\partial Y}=\frac{\alpha_{nf}}{\alpha_f}\left(\frac{\partial^2 \theta}{\partial X^2}+\frac{\partial^2 \theta}{\partial Y^2}\right)+\frac{(\rho c_p)_f}{(\rho c_p)_{nf}}Q\theta \quad (17)$$

The boundary conditions now take the following form:

$\tau<0: U=V=0,\ 0\le X\le 1,\ 0\le Y\le 1,$

On the left wall:

$\tau\ge 0: X=0,\ U=V=0, \frac{\partial\theta}{\partial X}=0, B\le Y\le 1-B, \theta=1,$ otherwise.

On the right wall:

$\tau\ge 0: X=1, U=V=0,\ \frac{\partial\theta}{\partial X}=0, B\le Y\le 1-B, \theta=0,$ otherwise.

On the bottom wall:

$\tau\ge 0: Y=0, U=V=0, \theta=1, 0\le X\le B, \theta=0, 1-B\le X\le 1, \frac{\partial\theta}{\partial Y}=0$ otherwise.

On the top wall:

$\tau\ge 0: Y=1, U=V=0, \theta=1, 0\le X\le B, \theta=0, 1-B\le X\le 1, \frac{\partial\theta}{\partial Y}=0$ otherwise.

Where

$$\Pr=\frac{\nu_f}{\alpha_f},\quad Ra=\frac{g\beta_f\,\Delta T\,H^3}{\nu_f\,\alpha_f},\quad Ha=B_0H\sqrt{\frac{\sigma_f}{\mu_f}},\quad B=\frac{b}{H},\quad Q=\frac{H^2}{k_f}Q_0 \quad (18)$$

are respectively the Prandtl number, Rayleigh number, Hartman number, and the dimensionless heat generation or absorption coefficient. *B* is the dimensionless the heat source/sink length.

The heat transfer rate across the enclosure is an important parameter in thermal system and its related applications. The local Nusselt number is defined as:

$$Nu_{L0}=-\frac{k_{nf}}{k_f}\left(\frac{\partial\theta}{\partial X}\right)_{X=0}, Nu_{L1}=-\frac{k_{nf}}{k_f}\left(\frac{\partial\theta}{\partial X}\right)_{X=0}$$
$$Nu_D=-\frac{k_{nf}}{k_f}\left(\frac{\partial\theta}{\partial Y}\right)_{Y=0}, Nu_T=-\frac{k_{nf}}{k_f}\left(\frac{\partial\theta}{\partial Y}\right)_{Y=1} \quad (19)$$

and the average Nusselt number is defined as:

$$Nu_{m1}=\frac{1}{B}\left(\int_0^B Nu_{L0}\,dY+\int_{1-B}^1 Nu_{L1}\,dY\right)$$

$$Nu_{m2}=\frac{1}{B}\int_0^B (Nu_D)_{Y=0}\,dX+\int_0^B(\mathrm{Nu}_T)_{Y=1}\,dX$$

$$Nu_m=\frac{Nu_{m1}+Nu_{m2}}{2} \quad (20)$$

3. NUMERICAL PROCEDURE

In the present study, the iterative finite difference method is used to solve the transient dimensionless governing equations (Eqs. (14)-(17)) subject to their corresponding boundary conditions given in Eq. (18). Approximation of convective terms is based on an second order upwind finite differencing scheme, which correctly represent the directional influence of a disturbance. The finite difference approximation for the heat equation can be expressed as follows:

$$\theta_{i,j}^{n+1}=\theta_{i,j}^n+\frac{\Delta\tau}{\sigma}\left\{\left(\frac{\alpha_{nf}}{\alpha_f}\right)\left[\frac{\theta_{i+1,j}^n-2\theta_{i,j}^n+\theta_{i-1,j}^n}{(\Delta X)^2}+\frac{\theta_{i,j+1}^n-2\theta_{i,j}^n+\theta_{i,j-1}^n}{(\Delta Y)^2}\right]+Q\frac{(\rho c_p)_f}{(\rho c_p)_{nf}}\theta_{i,j}^n-U_{i,j}^n\frac{\theta_{i+1,j}^n-\theta_{i-1,j}^n}{2\Delta X}-V_{i,j}^n\frac{\theta_{i,j+1}^n-\theta_{i,j-1}^n}{2\Delta Y}\right\}$$

where, i and j denote the cell locations. The equations (15), (16) and (17) can be approximated with the similar manner. A uniform grid resolution of 61×61 with a time step of 10^{-6} was found to be sufficient for all smooth computations and computational time required in achieving steady-state conditions.

4. RESULTS AND DISCUSSION

In this paper an iterative finite difference method is applied to obtain the numerical solutions of an unsteady MHD natural convection flow of a nanofluid in a cavity containing adiabatic obstacle with heated corners. The obstacle, placed in the middle of the cavity, is of square shaped and its size is controlled by the dimensionless of aspect ratio for square obstacle, *AR*. The boundary walls of the cavity are subject to the conditions prescribed in Eq. (18). Analysis has been done with the help of various ranges of the dimensionless parameters, which appear during formulation of the problem. These are: Rayleigh number, *Ra*, Hartman number, *Ha*, Prandtl number, Pr, heat generation or absorption coefficient, Q, nanoparticles volume fraction, ϕ, heat source length, B, and applied magnetic field angle, Φ .

In Figure **2** streamlines and isotherms are presented for different values of the dimensionless aspect ratio parameter, *AR*. In this figure the obstacle dimension increases from 0.1 to 0.5. In the streamlines contours, it is observed that two circulating cells are generated near the obstacle having dimension 0.1. These cells become stronger and takes dominant position when obstacle dimension increases from 0.1 to 0.5. As *AR* increases, the vortex become elliptic and finally breaks up into two vortices and settles down near the top and bottom faces of the cavity. It can be summarized that a central vortex may appear in case of no obstacle inside the cavity. In case of isotherms, the strength of the contours reduces when size of the obstacle increases from 0.1 to 0.5. For high *AR* intensified convective flow and heat transfer illustrate the temperature distribution in heated zones along the upper and lower walls of the cavity. Further, the profiles of average Nusselt number are displayed in Figure **3**. We may note that the average Nusselt number decreases considerably when size of the obstacle increases from 0.1 to 0.5.

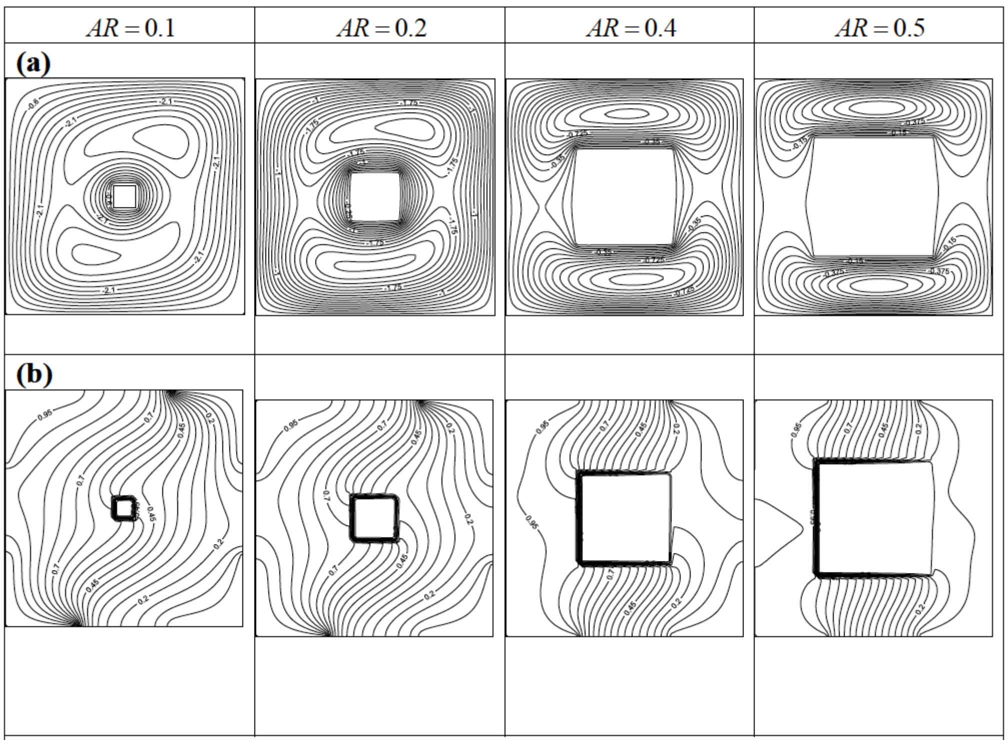

Figure 2: (**a**) Streamlines and (**b**) Isotherms for $\phi = 0.05, Ha = 10.0, B = 0.3,\ Q = 1.0, \Phi = \pi / 6,\ Ra = 10^4$

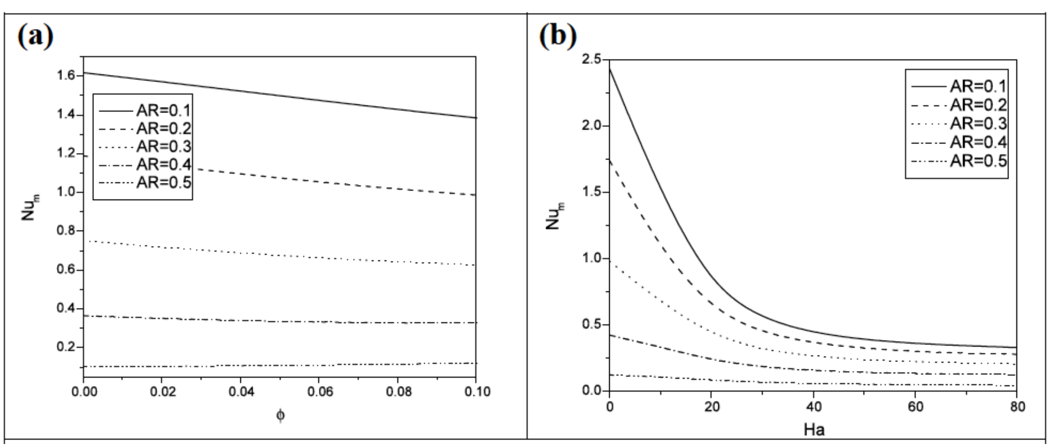

Figure 3: Variation of average Nusselt number with ϕ and *Ha* for different values of *AR*.

We see from Figure **4** that average Nusselt number (plotted against *Ha* and ϕ) increases as Ra increases. This is expected because of the convection dominated heat transfer.

Overall, the heat transfer rates diminish with an increase in heat generation parameter and it increases with an increases in the heat absorption parameter (negative values). This fact can be observed from the profiles of the average Nusselt numbers given in Figure **5**.

Due to an increase in temperature difference the buoyancy force decreases and the influence of shear-driven force increases. Further the variation of *B* in terms of local Nusselt number and average Nusselt number is presented in Figure **6**. Local Nusselt number is given against the streamwise and normal components whereas average Nusselt number are shown against ϕ and *Ha*. The magnitude of local and average Nusselt number decreases considerably for nanofluid suspension when B increases. This happens because the thermal conductivity of the nanofluid decreases and therefore local and average Nusselt number diminish considerably.

5. CONCLUSIONS

In this paper a square cavity is considered which contains an adiabatic square obstacle in its center. The novelty of the present work is to consider cavity containing a centered adiabatic square block as well as unsteady effects in the natural convection of nanofluids. The physical situation of the problem is described well in Figure **1**. Finite difference method is applied to solve the problem numerically and solutions are interpreted in terms of streamlines, isotherms, local Nusselt number and average Nusselt number. From this analysis it is observed that angle of applied magnetic field is important in the context that maximum rate of heat transfer can be achieved if transmitted along the *x*-axis and minimum can be transferred if applied along the *y*-axis. The graphs plotted for various values of Hartmann number shows that local Nusselt

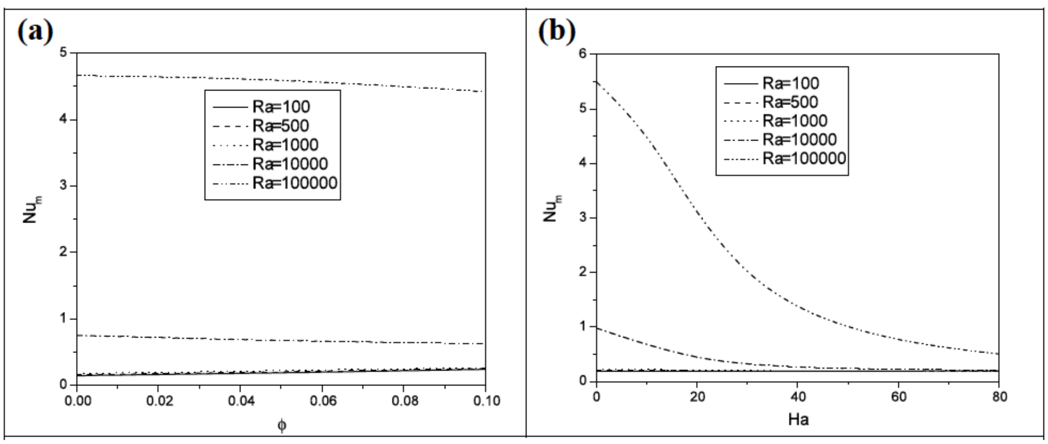

Figure 4: Variation of average Nusselt number with ϕ and *Ha* for different values of *Ra*.

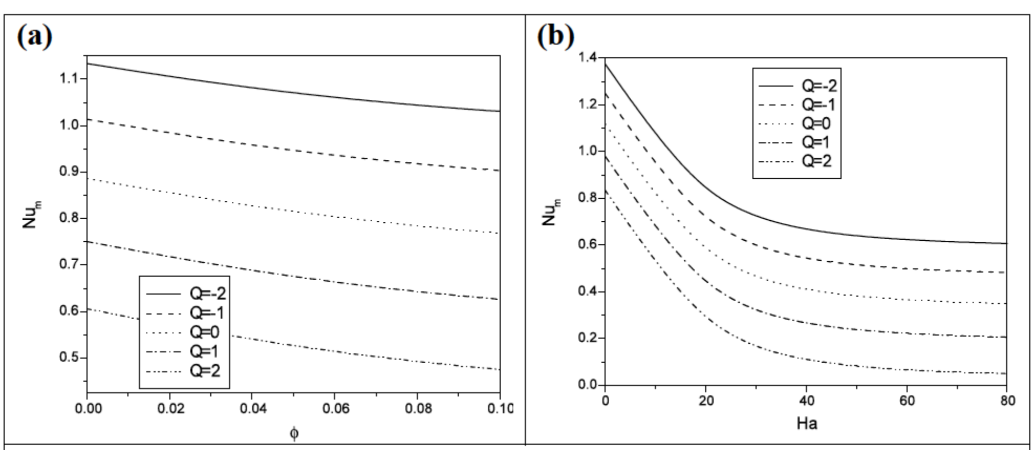

Figure 5: Variation of average Nusselt number with ϕ and *Ha* for different values of *Q*.

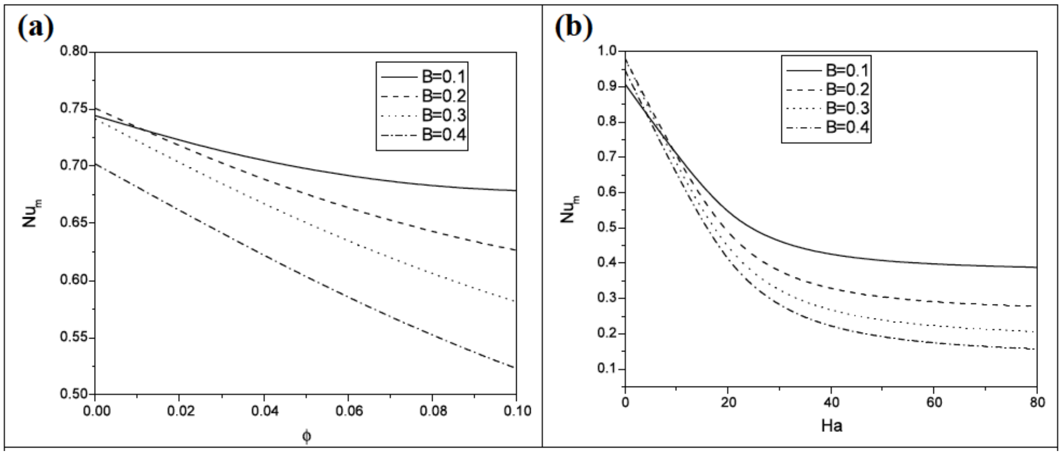

Figure 6: Variation of average Nusselt number with ϕ and *Ha* for different values of *B*.

number reduces along the heat source due to the Lorentz force. It is also observed that size of the adiabatic obstacle can extensively alter the flow pattern in the cavity. The heat transfer rate increases as the size of the obstacle increases. The Rayleigh number increases the heat transfer rate. The magnetic field angle does not influence the overall heat transfer rate significantly but has pronounced effect on streamlines of the flow. The magnetic field strength has pronounced effect on streamlines and isotherms, but reduces heat transfer rates. The nanoparticle volume fraction does not have significant effect on the shape of streamline cells formed within the cavity. The heat transfer rate decreases as the volume fraction increases.

Nomenclature	
B	heat source/sink length (m)
D	heat source/sink position (m)
g	gravitational field (m s^{-2})
H	cavity width (m)
Ha	Hartman number $Ha = BoH\sqrt{\alpha_f / \mu_f}$
Nu_s	local Nusselt number
Nu_m	average Nusselt number
p	pressure (N/m^2)
Pr	Prandtl number $\Pr = \nu_f / \alpha_f$
Q	Heat generation or absorption
Ra	Rayleigh number $Ra = g\beta \Delta T H^3 / \nu_f \alpha_f$
T	temperature (K)
u	velocity component along x-direction (m s^{-1})
v	velocity component along y-direction (m s^{-1})
V	dimensionless velocity component along y-direction
x,y	Cartesian coordinates (m)
X,Y	dimensionless Cartesian coordinates
Greek symbols	
α	thermal diffusivity (m^2 s^{-1})
β	thermal expansion coefficient (K^{-1})
ϕ	nanoparticles volume fraction
μ	dynamic viscosity (Pa.s)
ν	kinematic viscosity ($m^2 s^{-1}$)
θ	dimensionless temperature
ρ	density (kg m^{-3})
σ	electrical conductivity (S m^{-1})
Subscripts	
Al_2O_3	Alumina
bf	Base fluid
c	Cold
Cu	Copper
f	Fluid
h	Hot
m	Average
nf	Nanofluid

REFERENCES

[1] SUS. Choi, Enhancing thermal conductivity of fluids with nanoparticles. In: Proceedings of the 1995 ASME International Mechanical Engineering Congress and Exposition, FED 231/MD 1995; 66: 99-105.

[2] JA. Eastman, SUS. Choi, S. Li, W. Yu, LJ. Thompson, Anomalously increased effective thermal conductivities of Ethylene glycol-based nanofluids containing Copper nanoparticles. Appl. Phys. Lett 2001; 78: 718-720. https://doi.org/10.1063/1.1341218

[3] W. Yu, SUS. Choi, The role of interfacial layer in the enhanced thermal conductivity of nanofluids: a renovated Maxwell model. J. Nanoparticles Res 2003; 5: 167-171. https://doi.org/10.1023/A:1024438603801

[4] MA. Mansour, Sameh E. Ahmed, AM. Rashad, MHD natural convection in a square enclosure using nanofluid with the influence of thermal boundary conditions, Journal of Applied Fluid Mechanics, 2016; 9(5): 2515-2525. https://doi.org/10.18869/acadpub.jafm.68.236.24409

[5] AM. Rashad, RSR Gorla, MA. Mansour, SE. Ahmed, Magnetohydrodynamic effect on natural convection in a cavity filled with porous medium saturated with nanofluid, Journal of Porous Media 2017; 20(4): 363-379. https://doi.org/10.1615/JPorMedia.v20.i4.50

[6] J. Raza, A. Rohni and Z. Omar, "MHD Flow and Heat Transfer of Cu-water nanofluid in a semi porous channel," Intternational Journal of Heat and Mass Transfer 2106; 103: 336-340. https://doi.org/10.1016/j.ijheatmasstransfer.2016.07.064

[7] M. Azimi and R. Riazi, "MHD copper-water nanofluid flow and heat transfer through convergent-divergent channel," Journal of Mechanical Science and Technology 2016; 30: 4679-4686. https://doi.org/10.1007/s12206-016-0938-3

[8] AM. Rashad, MM. Rashidi, Giulio Lorenzini, Sameh E. Ahmed, Abdelraheem M. Aly, Magnetic field and internal heat generation effects on the free convection in a rectangular cavity filled with a porous medium saturated with Cu-water nanofluid, International Journal of Heat and Mass Transfer, 2017; 104: 878-889. https://doi.org/10.1016/j.ijheatmasstransfer.2016.08.025

[9] RSR. Gorla, S. Siddiqa, MA. Manosur, AM. Rashad, T. Salah, Heat source/sink effects on natural convection of a hybrid nanofluid-filled porous cavity, Journal of Thermophysics and Heat Transfer 2017; 31(4): 847-857. https://doi.org/10.2514/1.T5085

[10] MA. Mansour, S. Siddiqa, RSR. Gorla, AM. Rashad, Effects of heat source and sink on entropy generation and MHD natural convection of a Al2O3-Cu/water hybrid nanofluid filled with square porous cavity, Thermal Science and Engineering Progress, 2018; 6: 57-71. https://doi.org/10.1016/j.tsep.2017.10.014

[11] Aminossadati SM, Ghasemi B. Natural convection cooling of a localized heat source at the bottom of a nanofluid-filled enclosure. Eur. J. Mech. B/Fluids 2009; 28: 630-40. https://doi.org/10.1016/j.euromechflu.2009.05.006

[12] Khanafer K, Vafai K, Lightstone M. Buoyancy-driven heat transfer enhancement in a two dimensional enclosure utilizing nanofluids. Int. J. Heat Mass Transfer 2003; 46: 3639-53. https://doi.org/10.1016/S0017-9310(03)00156-X

[13] Abu-Nada E, Chamkha AJ. Effect of nanofluid variable properties on natural convection in enclosures filled with an CuO-EG-water nanofluid. Int. J. Therm. Sci 2010; 49: 2339-52. https://doi.org/10.1016/j.ijthermalsci.2010.07.006

[14] Maxwell JA. Treatise on electricity and magnetism. 2nd ed. Cambridge, UK: Oxford University Press; 1904.

[15] Brinkman HC. The viscosity of concentrated suspensions and solution. J Chem Phys 1952; 20: 571-81. https://doi.org/10.1063/1.1700493

Received on 30-7-2019 Accepted on 5-9-2019 Published on 14-9-2019

DOI: http://dx.doi.org/10.15377/2409-5826.2019.06.5